Numerical Simulation of High Temperature Corrosion Processes in Mn, Cr, Si, Al – Alloyed Steel Samples

M Auinger and M Rohwerder

Department of Interface Chemistry and Surface Engineering
Max-Planck-Institut für Eisenforschung, Max-Planck-Straße 1, D 40237 Düsseldorf, Germany

E-mail: auinger@mpie.de

Received:

Abstract

The grain boundary oxidation mechanism in hot rolled steel samples during cooling from 500 °C – 800 °C down to room temperature was mathematically modeled. Given a fixed temperature ramp, the migration of the atomic species (iron, oxygen and the alloying elements) has been calculated with the parabolic rate equation for diffusion. After each small time step, the data was transferred into the database ChemApp (GTT-Technologies, Germany) to calculate the oxide composition for each point in thermodynamic equilibrium.

The concentrations for each phase were illustrated in a phase map, similar to a cross section polish of the respective specimen. Total element concentration is shown as height plot to better pronounce the increased amount of oxidic phases along the grain boundaries.

The obtained results are in good agreement with experimental data for low alloyed steel samples.

1. Introduction

The binary phase diagrams of iron are one of the most intensively studied systems in industrial research [1] and due to their high importance in modern steel design, detailed descriptions of the phase stabilities are available.
However, in industrial manufacture of various steel parts, the alloy gets in contact with the atmosphere at already very high temperatures of up to 1 000 °C and oxides will be formed [2, 3]. Whereas the scaling (i.e. oxidation on the sample surface, mainly iron oxide) can be removed in order not to alter the metal forming process, inner oxidation along the grain boundaries and inside the grains is much more complicated to be influenced. Detailed descriptions of the alloy system in the presence of oxygen, are still not completed since most phase diagrams of the possible oxides of the alloying elements were studied for binary mixtures. Only little has been done for ternary or quaternary systems in the presence of iron oxides [4].

The aim of this work is to find an appropriate model to mathematically describe the process of internal oxidation in an alloyed steel sample at a given temperature program and to calculate the formed oxide phases.
These findings will further be compared with experimental results in order to determine the stability of (mixed) oxide phases as well as the migration behavior of the elements in the system.

2. Method Description

The description for the process of internal oxidation has been done in an alternating cycle of calculating the element migration and reaction. To give the reader a clearer overview of the essentials and to provide a better comparison with previous models [5, 6, 7] the microstructure of the steel sample was simplified to hexagonal grains of equal size, as illustrated in figure 1. To minimize calculation time, the smallest possible unit cell has been taken and the whole system can be reconstructed due to the periodic restrictions in the boundary conditions.

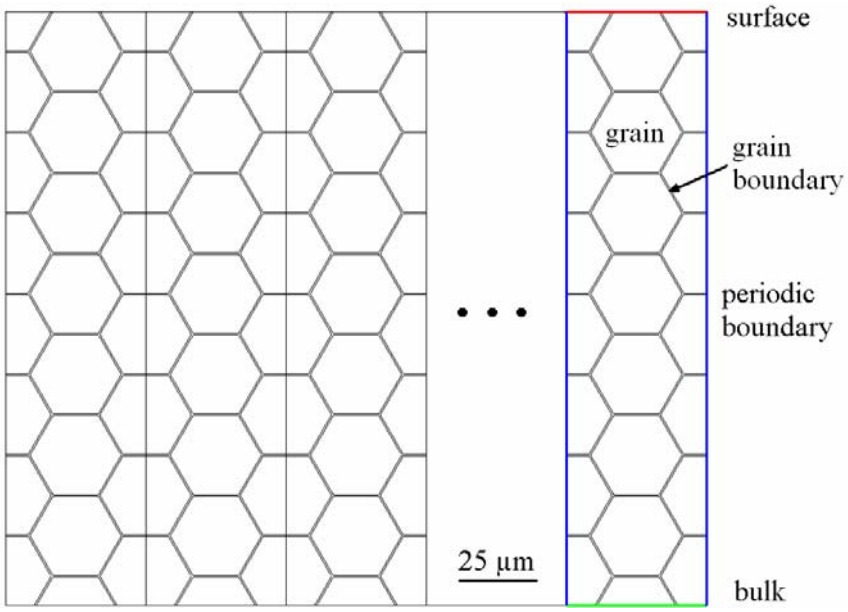

Figure 1: Microstructure and boundary conditions used throughout the simulations

The migration was considered for the atomic species (iron, oxygen and the alloying elements) by applying the parabolic rate equation for diffusion in the numerical software COMSOL (COMSOL Inc., USA). Within this model, the different tabulated temperature dependencies of the diffusion constant for the element in the grain (rather low value) and along the grain boundary (higher diffusibility) was taken into account [8, 9]. Existing oxide phases were considered to be immobile, so they were not computed in this short time step of the calculation.

Since oxidation is usually a very fast process, the chemical potential of atomic oxygen is very high and the activation energy for reaction can easily be overcome at elevated temperatures, the phases were considered to be in thermal equilibrium after each step of diffusion. Equilibrium calculations were carried out by an external link to the software ChemApp (GTT-Technologies, Germany) which returns the concentrations of the phases, taken into account at each numerical point of the simulation grid. These values were then used as starting point for the next iteration step.

The simulated temperature program, applied in this report consists of an initial isothermal step at 700 °C for 60 min, followed by a cool down to 300 °C with a constant rate of 40 °C h^{-1}. Results are usually displayed as a 2D concentration map for each considered phase, similar to a cross section polish of the alloy specimen. Three dimensional plots were only used to display

the total distribution of each element and to pronounce the differences between grain and grain boundaries.

3. Results and Discussion

The phase diagram in the left part of figure 2 shows the oxidation sequence with increasing oxygen partial pressure. In the present case of stainless steels, manganese is the first element to be oxidised, followed by chromium. On the right hand side of the figure, one can recognise the spatial distribution of all elements in the system. After completed cooling, it can be clearly seen that the amount in the grain boundaries first increased, followed by a depletion zone in close proximity to the maximum concentration. This results from the accelerated element transport along the boundary layers and the fact that the concentration gradient induces migration towards the surface of the sample. Since the diffusion constant in the bulk material is much smaller, compared to the grain boundaries, only little changes in the bulk composition could be observed.

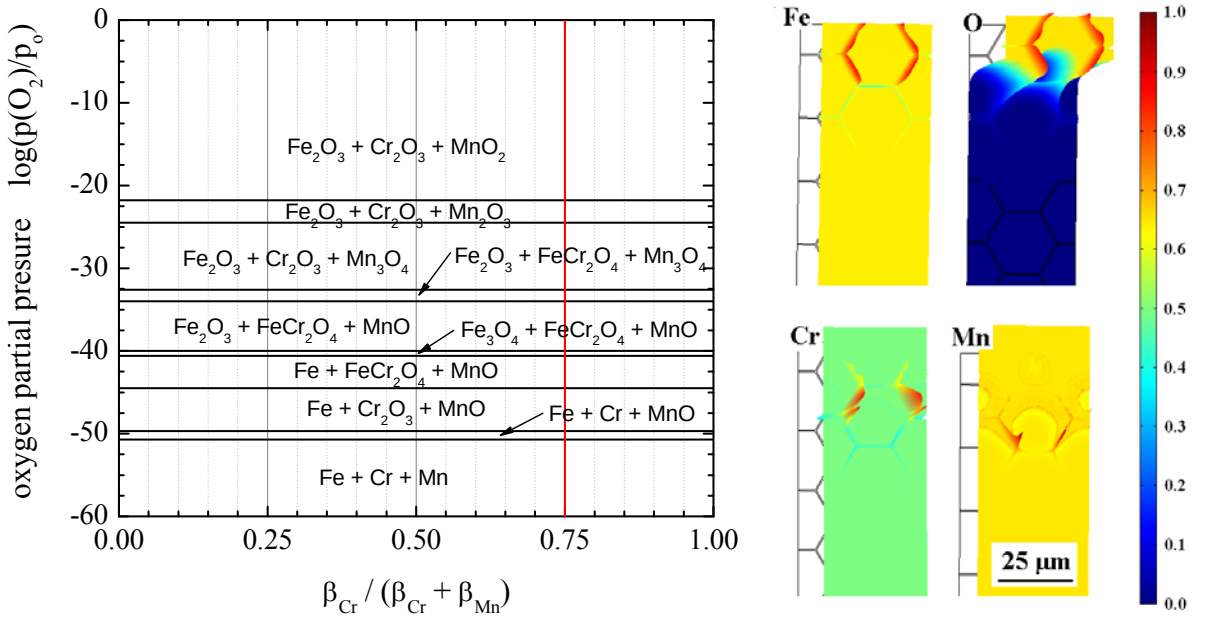

Figure 2: Thermodynamic stability diagram at 300 °C (left) and 3D element map in the system Fe-Cr-Mn, after completed oxidation (right). The red line in the left diagram shows the concentration Fe with 3 wt-% Cr, 1 wt-% Mn.

The concentration map of each phase in the steel reflects the systematic from the upper diagram. One can see the spatial distribution of the oxide phases, which corresponds to the average amount of each phase within a small sample volume. Experimentally, those oxide

phases are fine grained precipitates [10]. However, this was not taken into account in this simulation.

The distribution of chromium oxide in figure 3 shows the presence of 2 (3) spatially separated phases. Whereas the thin frontline and the small dot correspond to the initial formation of chromia, which then reacts with iron and oxygen to form the spinel-type $FeCr_2O_4$. The large area of Cr_2O_3 occurrence results due the decomposition of the iron-chromium oxide into Cr_2O_3 and Fe_2O_3.

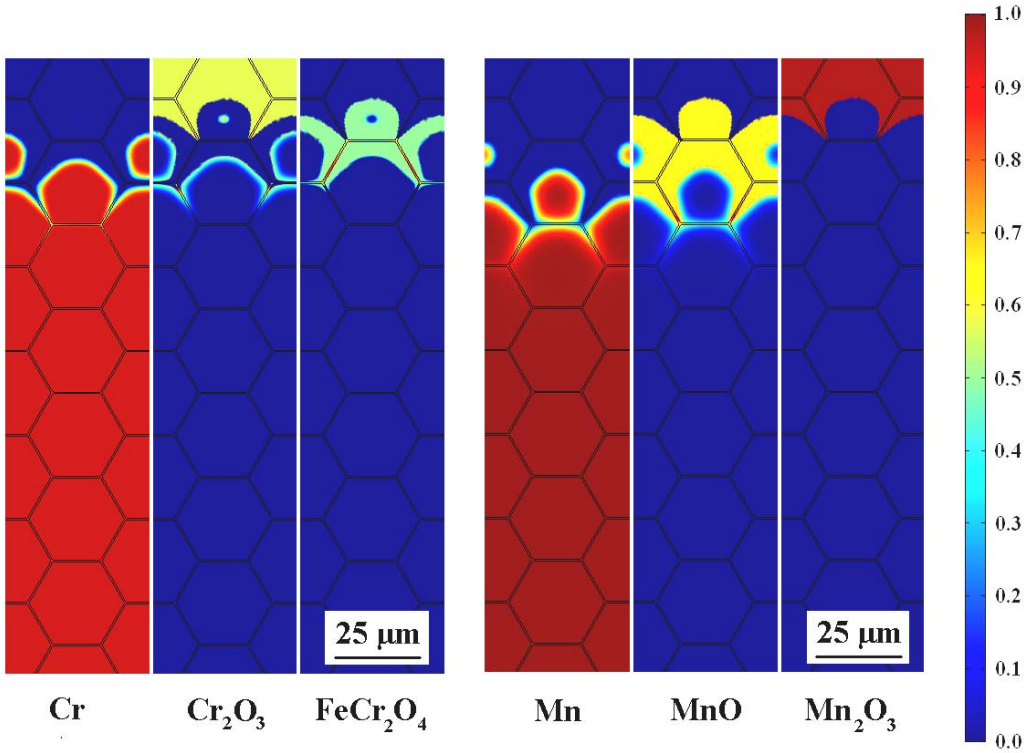

Figure 3: Spatial distribution of chromium and manganese phases in the system Fe-Cr-Mn after completed oxidation. The values are normalised to the maximum concentration of each phase.

Since manganese(II)oxide is the first oxidic phase to be formed in this system, its presence is a good indication for determining the total oxidation depth after the heat treatment. In the present case, the value ranges between 30 and 40 µm.

When changing the system from stainless steel to electrical steel i.e. use silicon and aluminium instead of chromium and manganese in the alloy, a similar accumulation of oxidic phases along the boundaries can be seen as in the previous case. Nevertheless, the oxidation scheme is slightly different due to the higher oxygen affinity of both silicon and aluminium.

In the present case, the total oxidation depth can be determined by the first occurrence of Al_2O_3, which again leads to values between 30 and 40 µm after completed heat exposure.

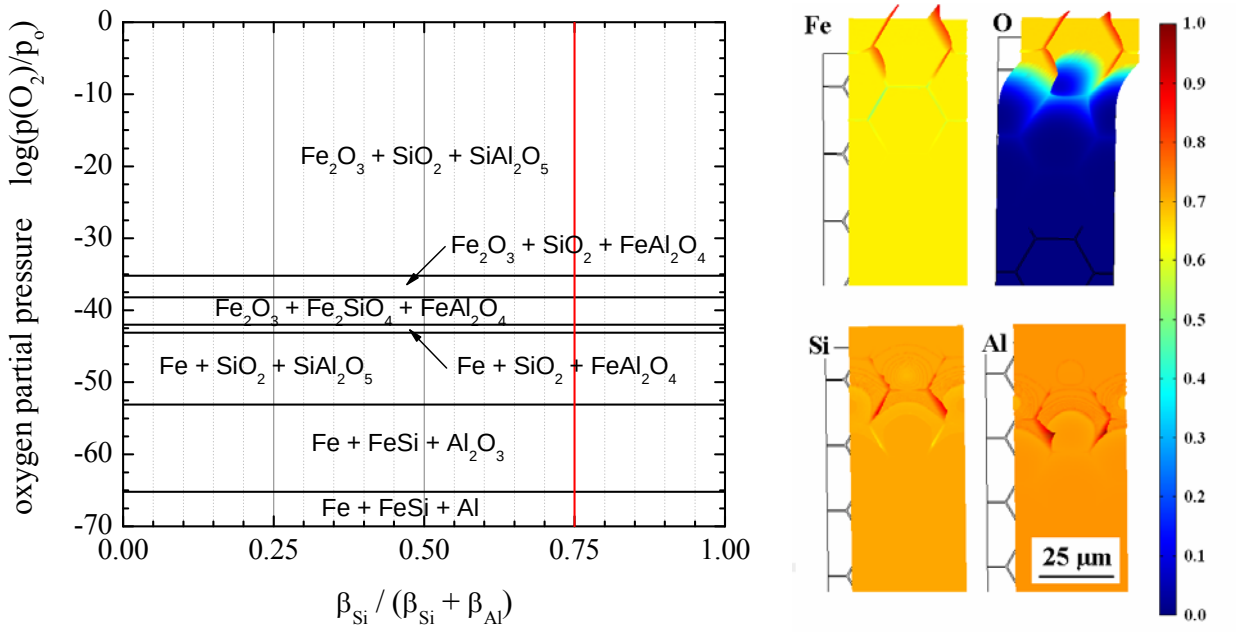

Figure 4: Thermodynamic stability diagram at 300 °C (left) and 3D element map in the system Fe-Si-Al, after completed oxidation (right). The red line in the left diagram shows the concentration Fe with 3 wt-% Si, 1 wt-% Al.

From the spatial distribution of the aluminium and silicon oxides in figure 5, the oxidation first starts to form the pure oxides Al_2O_3 and SiO_2 (calculated as β-quartz). By further increasing the oxygen partial pressure, iron gets oxidised and forms the compounds $FeAl_2O_4$ and Fe_2SiO_4 which finally decompose into the original alumina and silicon oxide phases.

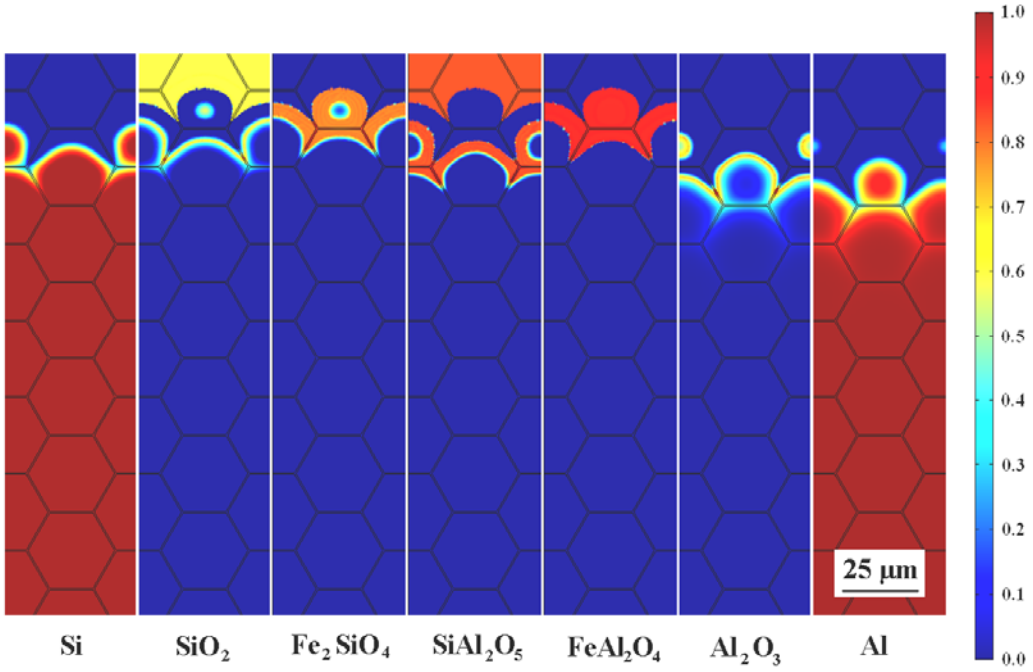

Figure 5: Spatial distribution of silicon, aluminium and oxidic phases in the system Fe-Si-Al after completed oxidation. The values are normalised to the maximum amount of each phase.

Concerning thermodynamic data and the fact that there is more silicon in the alloy than aluminium, alumina and silica combines to $SiAl_2O_5$ (andalusite) until all the aluminium oxide as limiting phase has been consumed. Thus the presence of two separated andalusite domains in the upper distribution can be monitored.

4. Conclusion

The above described procedure gives a good understanding of experimental findings in high temperature corrosion processes in low alloyed steel samples [3]. Deviations from this approach can be observed, when the amount of alloying elements exceeds a certain limit where the formation of a passive oxide layer is observed. This protects the sample from further oxygen attack and is the basic of high temperature corrosion protection.

A description of element migration by using a concentration gradient strictly works only for single phases. More correctly, the system may be described by using the gradient of the partial chemical potential rather than concentration. Herewith, segregation phenomena between grain and grain boundaries would be taken into account as well.

Furthermore, more detailed measurements of the temperature dependence of the migration constants in each chemical phase need to be carried out since the transport mechanisms along the grain boundaries are still a matter of research. Further work on this topic needs to be done.

Acknowledgement

The authors gratefully acknowledge the fundings by the Christian Doppler Forschungsgesellschaft and the voestalpine AG as part of the project “Diffusions- und Segregationsvorgänge bei der Produktion hochfesten Stahlbands”.

References

[1] B. Predel, M. Hoch, M. Pool, *Phase Diagrams and Heterogeneous Equilibria - A Practical Introduction*, Springer-Verlag Berlin (2004)

[2] W.F. Hosford, R.M. Caddell, *Metal Forming – Mechanics and Metallurgy*, Third Edition, Cambridge University Press (2007)

[3] V.P. Deodeshmukh, S.K. Srivastava, *J. Mater.* **7** (2009) 56-59

[4] F.J.M. Rietmeijer, J.M. Karner, J.A. Nuth-III and P.J. Wasilewski, *Eur. J. Mineral.* **11** (1999) 181-186

[5] J.C. Fisher, *J. Appl. Phys.* **22** (1951) 74-77

[6] S.N. Basu, J.W. Halloran, *Oxid. Met.* **27** (1987) 143-155

[7] U. Krupp, V.B. Trindade, P. Schmidt, H.J. Christ, U. Buschmann and W. Wiechert, *Mater. Corros.* **56** (2005) 785-790

[8] D. Gryaznov, J. Fleig, J. Maier, *J. Appl. Phys.* **103** (2008) 063717

[9] H. Bakker, H.P. Bonzel, C.M. Bruff, M.A. Dayananda, W. Gust, J. Horv'ath, I. Kaur, G.V. Kidson, A.D. LeClaire, H. Mehrer, G.E. Murch, G. Neimann, N. Stolica, N.A. Stolwijk, *Landolt-Börnstein: Numerical Data and Functional Relationships in Science and Technology*, Volume 26: Diffusion in Solid Metals and Alloys, Springer-Verlag Berlin Heidelberg (1990)

[10] W.J. Quadakkers, J. Żurek, M. Hänsel, *J. Mater.* **7** (2009) 44-50